

Irreversible Sorption of Neutral Hydrocarbons to Sediments: Experimental Observations and Model Predictions

A. T. KAN,* G. FU, M. HUNTER,[†]
W. CHEN, C. H. WARD, AND
M. B. TOMSON

Hazardous Substance Research Center/South & Southwest,
Department of Environmental Science and Engineering,
MS-317, Rice University, Houston, Texas 77005

Contaminants of environmental concern commonly reside in the sediment or solid phase. The extent and rate of desorption has heretofore been particularly unpredictable. In the present research, the adsorption and desorption of seven organic compounds with water solubilities ranging from 0.005 to 517 mg/L have been studied in natural sediments. In every case, a fraction of the adsorbate was adsorbed irreversibly (i.e., desorption was not the opposite of adsorption, yet the sorbate is not covalently bonded to the sediment). Each sediment-contaminant combination exhibited a fixed maximum irreversible adsorption, q_{\max}^{irr} , which could be filled in one or several steps and which is related to common molecular properties and sediment organic carbon content (OC). For most compounds, q_{\max}^{irr} ($\mu\text{g/g}$) $\approx 10^{3.8\text{OC}}$. Furthermore, the OC-normalized partition constant for this irreversible compartment is essentially constant for the compounds and sediments studied with $K_{\text{OC}}^{\text{irr}} = 10^{5.53 \pm 0.48}$ mL/g. After about 1–3 days of contact time, all laboratory adsorption and desorption data could be modeled using a single isotherm equation, based upon commonly measured chemical and sediment parameters. The isotherm equation consists of two terms, a linear term to represent reversible sorption and a Langmuir-type term to represent irreversible sorption. This combined isotherm is used to interpret numerous published field studies. The potential impact of this model on sediment quality criteria (SQC) and remediation are discussed.

Introduction

Chemical desorption from soil and sediment is of central importance to most environmental concerns. Desorption affects chemical fate, toxicity, and associated risk to human and aquatic life as well as the efficiency of most remediation technologies. Desorption is commonly modeled as a reversible partitioning process in fate, risk, and remediation models (1). However, the reversible model has failed to predict the long-term persistent release of contaminants to the environment. Even with the most advanced remediation technologies (physically, chemically, and/or biologically enhanced),

it is often observed that a small fraction of the sorbed contaminant remains in the soil or sediment unexpected. The existence of this remaining fraction has hindered the closure of many cleanup operations. Knowledge and prediction of desorption is necessary for designing more effective remediation schemes. If it could be shown that pollutants would not be released from sediments in any significant concentrations, either abiotically or via biological means, they would be of little practical concern and could be safely left in place. In this case, the impact on remediation costs could be enormous.

Numerous theories have been proposed to explain the existence of this resistant fraction. Recent research by the authors has shown that a significant fraction of some contaminants is bound into sediments irreversibly [i.e., desorption is not the opposite of adsorption (2–5)]. The irreversible compartment can be filled stepwise in multiple adsorption/desorption steps (5). After the maximum capacity is reached, subsequent adsorption/desorption steps are completely reversible. The term “irreversible” used herein is in the same manner as is commonly used in the physical-chemical literature, e.g., Adamson (6), Bailey et al. (7), and Burgess et al. (8). A minimum thermodynamic requirement for adsorption and desorption to be irreversible is that there be a physical-chemical rearrangement in the solid phase after adsorption occurs, i.e., the desorption takes place from a different molecular environment than that in which adsorption occurs (6). Adamson (6) has summarized a number of well-known systems (e.g., aqueous dyes with TiO_2 and SiO_2 , and alkane adsorption on activated charcoal) in which adsorption irreversibility has been observed.

In addition to irreversible adsorption, several other mechanisms have also been proposed to explain the observed resistant desorption. For several classes of organic and inorganic compounds, chemisorption is the cause for the resistant release of chemicals from sediments and soil (9). However, chemisorption is limited to specific classes of pollutants and usually is not a major consideration for most neutral hydrophobic organic chemicals, which are considered in this paper (9). Heterogeneous adsorption with varied adsorption sites has been proposed to explain the persistent release of contaminants, whereby a fraction of the chemical is assumed to adsorb to sites with high adsorption energy or specificity, e.g., soot, a condensed soil organic phase or specific adsorption sites on an organic polymer, etc. (10–12). Heterogeneous adsorption isotherms often deviate significantly from linearity.

Another group of scientists has proposed that the resistant fraction is a result of unusually slow time-dependent processes (13–15). In previous studies, the authors have compared the time-dependent sorption rate of naphthalene and phenanthrene on Lula sediments (3). It was observed that approximately 50% of the total mass in a phenanthrene experiment was partitioned onto the solid phase within the first minute of reaction time. Such a rapid adsorption rate is typical for physical adsorption (16). Approximately 80% of the total mass was adsorbed after 4 h in both the naphthalene and phenanthrene experiments. This second time-dependent sorption of these two compounds to Lula sediments can be modeled with the retarded intraparticle radial diffusion model (17). The resulting apparent diffusion coefficients are 3.5×10^{-8} cm^2/s for naphthalene and 8×10^{-10} cm^2/s for phenanthrene. The apparent diffusion coefficients of 2×10^{-8} and 1.3×10^{-9} cm^2/s can also be estimated independently for naphthalene and phenanthrene respectively, based on the molecular diffusion coefficient (6

* Corresponding author: Phone: (713) 285-5224; fax (713) 737-5660; e-mail: atk@rice.edu.

[†] Present address: Department of Engineering, Hofstra University, Hempstead, NY 11550.

$\times 10^{-6}$ cm²/s), partition coefficients, and assuming an intraparticle porosity of 0.13 (18). The experimental values are in good agreement with the calculated values. Considering these diffusion rate constants, the equilibrium time of 1 day to 1 week would be calculated for compounds and sediments used in this research. It is still possible that extremely slow diffusion is not detected in such short reaction times.

Diffusion of organic compounds into either constricted microporous channels or glassy/crystalline organic phase have been proposed, and adsorption and desorption times of years are possible with these extremely slow diffusion rates (13–15). Both heterogeneous adsorption and slow diffusional processes will be considered in the following desorption studies.

Several unique features of the resistant desorption have been reported in the literature. First, a fraction of the sediment phase contaminants persists over tens of years without significant reduction in concentration (19, 20). Second, the solution phase concentration often remains much lower than expected from equilibrium partitioning with the solid-phase concentration (21–23). Third, there is a poor correlation between the field-observed partition coefficient and the predicted equilibrium partition constant, K_p , derived from conventional K_{OC}/K_{OW} relationships (20, 21). For contaminants with several orders of magnitude differences in solubilities, a constant partition coefficient (K_{OC}) has been reported for desorption from this resistant fraction (24–27).

The overall objective of this research is to develop a predictive correlation to model contaminant release for both laboratory and field observations. A semiempirical irreversible sorption isotherm model, based on the laboratory observed parameters, has been developed and used to correlate most field observations reported in the literature. Chemicals used in this study include an aromatic compound (toluene), a halogenated aromatic compounds (1,2 dichlorobenzene), two polycyclic aromatic hydrocarbons (PAHs), two polychlorinated biphenyls (PCBs), and a chlorinated pesticide (DDT). Several types of sediments containing various organic carbon contents have been tested.

Materials and Methods

Sorbent. Four sediments were used in this study. Three sediments (Lula, Dickinson, and Utica), were used for exhaustive adsorption and desorption studies to saturate and study the irreversible compartment; one sediment, from Lake Charles, was already heavily contaminated with chlorinated compounds and was primarily used for studies of sediment phase contamination. The properties of Lula and Dickinson sediments have been reported previously (2, 5, 28). The Utica sediment is the bottom sediment collected from Utica Harbor near a gas manufacturing plant. Both Lula and Dickinson sediment samples used in this study did not contain a detectable quantity of hydrocarbon pollutants (28, 29), even though the Dickinson Bayou should have received chemical input from both Urban and industrial sources surrounding Texas City, Texas. The Utica sediments were contaminated with a number of polycyclic aromatic hydrocarbons (PAHs). The Lake Charles sediment is the bottom sediment collected in 1995 near the outfall of an industrial canal that flows into Bayou d'Inde, Lake Charles, LA. The Lake Charles sediment is contaminated with chlorinated aromatic compounds and petroleum contaminants. The sediments from similar area has been characterized extensively since 1985 (19, 30, 31). The organic carbon content of the Lula, Dickinson, Utica, and Lake Charles sediments is 0.27, 1.50, 1.07, and 4.10%, respectively.

Sorbate and Chemicals. The following seven radiolabeled [¹⁴C] compounds were obtained from Sigma and used as

TABLE 1. Typical Experimental Protocols: Two Phenanthrene Experiments^a

I. Phenanthrene Experiment P–2 (See Figure 1a)

1. 8 adsorptions followed by six desorptions

adsorption	1–3 days per step ~98% supernate was replaced with Phen solutions $C_{\text{initial}} = 0.239\text{--}0.713 \mu\text{g/mL}$
desorption	1–3 days per step ~65% supernate was replaced with clean electrolyte
2. 9th adsorption followed by six desorptions

adsorption	1 day; $C_{\text{initial}} = 0.290 \mu\text{g/mL}$
desorption	1–3 days ~65% supernate was replaced with clean electrolyte
3. 10th adsorption followed by eight desorptions

adsorption	1 day $C_{\text{initial}} = 0.393 \mu\text{g/mL}$
desorption	1–3 days ~65% supernate was replaced with clean electrolyte

II. Phen Experiment P–4 (See Figure 1b)

1. 4 adsorption followed by 49 desorptions

adsorption	1–4 days ~96% supernate was replaced with Phen solutions; $C_{\text{initial}} = 0.454\text{--}0.532 \mu\text{g/mL}$
desorption	1–59 days ~90% supernate was replaced with clean electrolyte

^a Solution matrix: 1 mM CaCl₂·2H₂O, 0.1 mM MgCl₂, 0.5 mM Na₂B₄O₇·10H₂O (pH 8.0), 10 mM formaldehyde. Solid/solution ratio: 2 g of Lula sediments, 23.3 mL of electrolyte solution. Mixing: Horizontal shaking at about 60 times/min.

sorbates (abbreviation and specific activity in microcurie per micromole): (1) toluene (Tol, 9.7); (2) naphthalene (Naph, 8.9); (3) 1,2-dichlorobenzene (Cl₂-Ben, 10.7); (4) phenanthrene (Phen, 8.3); (5) 4,4'-dichlorobiphenyl (Cl₂-PCB, 13.8); (6) 2,2',5,5'-tetrachlorobiphenyl (Cl₄-PCB, 12.2); and (7) 1,1-bis(*p*-chlorophenyl)-2,2,2-trichloroethane (DDT, 13.4). The purities of Tol, Naph, Cl₂-Ben, Cl₄-PCB, and DDT have been confirmed in the laboratory by GC. The [¹⁴C]Tol, Naph, and Cl₂-Ben were further diluted with unlabeled ¹²C stock solution (76 958, 1500, and 3775 mg/L in methanol, respectively, for Tol, Naph, and Cl₂-Ben) to yield a specific activity of 0.32, 2.262, and 3.742 μCi/μmol, respectively. Formaldehyde (0.01 M) or sodium azide (0.01 M) was added to the solution as a bacterial inhibitor. Chemical solution was prepared in buffered solution (pH 8.0) before each adsorption experiment using the ¹⁴C stock solution and electrolyte solution containing 1 mM CaCl₂·2H₂O, 0.5 mM MgCl₂, 1 mM Na₂B₄O₇·10H₂O (pH 8). The amount of methanol and formaldehyde added to the vials constitutes less than 2% (v/v) or 1% (mole fraction) of the liquid, which should not affect the cosolvent properties of the liquid phase significantly (32).

Batch Adsorption and Desorption Experiments. A total of seven chemicals and three sediments have been tested with the multiple cycles of adsorption/desorption experiments, similar to that of Kan et al. (5). An adsorption/desorption cycle refers to a series of 1–8 successive adsorptions followed by 5–89 successive desorptions. Each data set is the result of multiple adsorption/desorption cycles of up to 120 individual experiments. Table 1 lists two typical experimental procedures with Phen, as an example. The other experiments are similar to one of these experiments with some variations discussed below. The adsorption/desorption experiments were typically conducted in a batch

reactor, which consisted of a glass vial of total volume approximately 7 mL (Tol experiments), 26 mL (Naph, Cl₂-Ben, Phen, Cl₂-PCB, and DDT experiments) and 40 mL (Cl₄-PCB experiments) sealed with Teflon-faced silicone septa (Wheaton). Control experiments were run with the vials containing Naph solution at 1 µg/mL to test the integrity of the vial. Since these chemicals have the tendency to adsorb to glasswares, either carefully cleaned glasswares (4) or the preclean, EPA-certified vials (Fisher Scientific) were used. The adsorption of hydrophobic organic chemicals to clean glass surfaces are minimal. Typically, less than 5% reduction of the solution-phase concentration was observed in the controls over a 30 day period.

At the beginning of the adsorption experiments, dried sediment (0.1–2 g) was added to the vial before the addition of chemical solution at concentrations from 112 to 237 mg/L for Tol; 3 to 15.1 mg/L for Naph; 1.0 to 35.3 mg/L for 1,2 Cl₂-Ben, 0.390 to 0.713 mg/L for Phen, 0.166 to 0.342 mg/L for Cl₂-PCB, 0.009–0.013 µg/mL for Cl₄-PCB, and 0.053 to 0.098 mg/L for DDT. After filling with sediment and solution, the vial typically contained a very small headspace of less than 0.1 mL. The sediment/water mixture was horizontally mixed in a shaker bath at room temperature. After 1–7 days, the sediment was separated from solution by centrifugation at a centrifugal force of 300g for 15 min (International Clinical Centrifuge, W. H. Curtin Co.) and the chemical concentration in the supernate was analyzed. Numerous other centrifugation rates and separation methods were tested with no appreciable effect (3). For Phen, Cl₂-PCB, and DDT experiments, the sediments were either spiked with the chemical stock solution or replaced with another aliquot of the chemical solution, and the adsorption experiments were repeated 4–9 times before desorption began. After adsorption, desorption was induced by successively replacing 60–95% supernatant with contaminant-free electrolyte solution. The incubation period for desorption experiments was typically from 1 to 3 days with exceptions where various incubation periods from 1 h to 6 months were used. After the successive desorption steps, the solution was decanted and wet sediment was left in the bottle with about 0.5 mL of liquid remaining (actual amounts were determined by weight). An aliquot of chemical solution was added to the vial to conduct another cycle of adsorption/desorption experiments. Both Naph/Lula and Phen/Lula experiments have been repeated with varying initial chemical concentrations and varying solid/solution ratios from 1/12 to 1/240 (wt/vol) with similar results.

The cycles of adsorption/desorption were repeated until the desorption reversibility for the last adsorption/desorption cycle was observed, i.e., the amount adsorbed in the last adsorption step desorbed reversibly as one would predict using the linear partitioning model and the measured adsorption K_p value (see eq 1 below). The solid-phase Naph, Cl₂-Ben, Phen, Cl₂-PCB, and Cl₄-PCB concentrations in Lula sediments were measured at the end of the adsorption/desorption steps by methylene chloride extraction, where solvent was refluxed in a round-bottom flask containing sediment for 24 h in a constant temperature water bath at 45 °C (3). A second methylene chloride extraction was done with one of the experiments, and no additional mass was extracted. The extraction efficiency of this procedure is typically better than 95% (2). The concentration of chemicals recovered from the solvent extraction was quantified by scintillation counting. The chemical was also identified by GC/MS analysis.

The solution-phase chemical concentrations were determined by scintillation counting (Beckman LS3801) using Beckman ReadySafe scintillation cocktail. The concentrations of chemicals in both the liquid and solid phases are within the sensitivity of scintillation counting. At counting

times of 10 min/sample, the 95% confidence interval of the counting efficiency is about ±5% at 0.000 635 µg/mL and ±9.8% at 0.000 027 µg/mL for Cl₄-PCB. The solid-phase chemical concentrations were calculated by assuming that the changes in solution-phase concentrations during adsorption or desorption were equal to the changes in solid-phase concentration. The solid-phase chemical concentration in Utica and Lake Charles sediments were extracted with methylene chloride by Soxhlet extraction and analyzed on GC. The chemical in the solid extract was also analyzed with GC/MSD (HP 5890/5970) for positive compound identification.

Results

Cyclic Adsorption/Desorption Studies of Phenanthrene.

Cyclic adsorption and desorption experiments were done with seven different compounds chosen to span a wide range of K_{OW} values following the procedure similar to Naph/Lula experiments reported by Kan et al. (5). Previous experiments have shown that the irreversible compartment can be filled in one step if the solution-phase concentration at equilibrium is greater than about one-third to one-half of the aqueous solubility (C_{aq}^{sat}) (5). In the following, two Phen experiments are discussed in detail to illustrate the typical result. Similar results regarding the solid and solution phase concentrations of the irreversible compartment were observed with other chemicals and sediments and the data are summarized in Table 2. Desorption times of 1 h to 6 months were used to determine the equilibrium and kinetic aspects of desorption from the irreversible compartment.

Figure 1 shows typical multiple cycle adsorption and desorption data using Phen [experiments (exps) P-2 and P-4]. Figure 1a is a plot of the solid versus solution-phase concentration of Phen during adsorption and desorption (exp P-2). The adsorption data can be modeled with simple linear isotherm (eq 1):

$$q = K_p \cdot C \quad (1)$$

where q (µg/g) is the solid-phase concentration and C (µg/mL) is the solution-phase concentration, K_p (mL/g) is the linear isotherm partition coefficient. The linear partition coefficient, K_p , can be normalized to the soil organic carbon content, K_{OC} (33):

$$K_{OC} = K_p / OC \quad (2)$$

The first seven successive adsorption steps follow a linear isotherm with a log K_{OC} of 4.08, which is reasonable for Phen with a log K_{OW} of 4.57. The eighth adsorption step deviates from the linear adsorption isotherm. This is possibly because the equilibrium concentration is in excess of one-third of the saturation, ~1.1 µg/mL (34). The subsequent desorption deviates significantly from the adsorption isotherm. The second cycle of adsorption/desorption begins with the ninth adsorption step, which deviates from the linear adsorption isotherm, since a significant mass of Phen resists desorption from the previous cycles. In fact, the ninth adsorption datum would fall on the linear adsorption isotherm line if Phen in the resistant fraction is subtracted from the solid-phase concentration, i.e., Phen in the irreversible compartment is not competing with the newly added Phen for adsorption. The additional mass adsorbed in the ninth adsorption step was completely desorbed in the subsequent six desorption steps, i.e., the adsorption and desorption are reversible following the ninth adsorption step. Another cycle of adsorption/desorption was done (adsorption no. 10) and reversible adsorption/desorption was again observed, i.e., the Phen adsorbed in adsorption no. 10 desorbed to within experimental error. At the end of exp P-2, 7.9 µg/g Phen was

TABLE 2. Summary of Laboratory-Observed Adsorption Partition Coefficients, Equilibrium Solution and Solid-Phase Concentrations of the Irreversible Compartment at Maximum Capacity, the Irreversible Fraction Partition Coefficient Normalized per OC ($\log K_{OC}^{irr}$, mL/g)

sediment	chemicals	K_p^a (mL/g) (<i>r</i>)	$\log K_{OC}$	$C(\max)^b$ ($\mu\text{g/mL}$) (std dev)	q_{\max}^{irr} ($\mu\text{g/g}$)	$\log K_{OC}^{irr}$ (mL/g) (std dev)	no. of data	eq time (days)
Lula	ToI	0.4	2.17	0.138 (0.027)	125	5.31 (0.22)	3	8–10
Lula	Naph	2.19 (0.999)	2.91	0.003 49 (0.000 06)	10.95 ^{c,d}	6.05 (0.03)	5	3–29
Lula	Cl ₂ -Ben	3.65	3.13	0.0204 (0.0045)	44±7 ^c	5.50 (0.40)	4	3–5
Lula	Phen	32.66 (0.943)	4.08	0.001 11 (0.000 15)	7.9 ^c	6.38 (0.08)	18	3–59
Lula	Cl ₂ -PCB	141.6 (0.944)	4.71	0.009 54 (0.000 50)	5.9 ^c	5.38 (0.01)	3	4–11
Lula	Cl ₄ -PCB	59.07	4.34	0.000 64 (0.000 03)	0.36 ^{c,d}	5.50 (0.18)	20	1–26
Lula	DDT	187.8 (0.991)	4.84	0.0023 (0.0018)	1.75	5.76 (0.31)	9	3–18
Dickinson	ToI	2.46	2.22	0.213 (0.0154)	134	4.58 (0.11)	3	1–5
Dickinson	Naph	15.17 (0.998)	3.00	0.006 (0.0019)	72	5.83 (0.10)	3	8–10
Dickinson	DDT	598.0 (0.996)	4.60	0.002 03 (0.000 28)	10	5.29 (0.23)	6	4–36
Utica	DDT	407.5 (0.986)	4.58	0.001 88 (0.000 46)	5	5.23 (0.16)	6	4–36
overall mean and standard deviation						5.53 ± 0.48		

^a Adsorption partition coefficient. Number in parentheses is the correlation coefficient of the data fit to the linear isotherm (eq 1). ^b $C(\max)$ refers to the concentration at equilibrium when the irreversible compartment is saturated with q_{\max}^{irr} . ^c These values of q_{\max}^{irr} were determined by solvent extraction of the solid. ^d Data from Kan et al. (5).

expected in the irreversible compartment, based on mass balance calculations. The solvent extraction of the solid yielded 7.7 $\mu\text{g/g}$ Phen, indicating an excellent mass balance of 98%. In this experiment, a maximum irreversible solid-phase concentration ($q_{\max}^{irr} \approx 7.7\text{--}7.9 \mu\text{g/g}$) is reached in the first cycle of adsorption/desorption experiments, since the subsequently added Phen can be easily desorbed.

In Figure 1b is a plot of the adsorption/desorption isotherm for exp P-4 wherein the irreversible compartment has been saturated, based upon exp P-2. Similar resistant fraction (7.4 $\mu\text{g/g}$) was observed in this experiment. In Figure 1c is a plot of the solution phase concentration, C ($\mu\text{g/mL}$) of exp P-4 versus desorption step number for steps 25–49 following the fourth adsorption shown in Figure 1b. Only the data with desorption times greater than 3 days are plotted. The numbers on the plot indicate the range of equilibrium times (in days) used in individual desorption experiments. Small variations in solution phase concentrations (1.11 ± 0.15 $\mu\text{g/L}$) are observed in these desorption steps, where desorption times range from 3 to 59 days. These data in Figure 1c infer that desorption from the irreversible compartment may reach equilibrium at a concentration lower than predicted from the conventional K_{OC}/K_{OW} relationship. Figure 1d shows the partition coefficient (K_p) measured from the desorption data versus adsorption/desorption step number for this experiment. Note that K_p increases by about 200-fold (from about 33 to 6477) during successive desorptions. The value of K_p increases to a plateau within about 25 steps and remains nearly constant for subsequent desorptions.

Irreversible Fraction Partition Coefficient, K_{OC}^{irr} . In Table 2 is listed 11 adsorption/desorption experiments with seven chemicals and three sediments. For each experiment, the adsorption partition coefficients, K_p and K_{OC} , a maximum irreversible capacity (q_{\max}^{irr} , $\mu\text{g/g}$), a constant solution phase concentration (C , $\mu\text{g/mL}$) at equilibrium with the maximum irreversible compartment, and a constant OC normalized

partition coefficient, (K_{OC}^{irr} , mL/g), at equilibrium with the irreversible compartment, are reported with standard deviations in parentheses. K_{OC}^{irr} is defined similarly as in eq 2, where the partition coefficient is the ratio of the organic carbon normalized solid-phase and solution-phase concentrations after extensive desorption (which is typically after 20 desorption steps). As shown in Figure 1d, K_{OC}^{irr} is a constant since K_p of desorption reaches a constant that is different from the K_p of adsorption (Figure 1d). In columns 8 and 9 of Table 2, the number of data points and the range of desorption equilibrium times (days) used in the experiments are listed for reference. Most of the measured adsorption K_{OC} values are within a factor of 2 of $K_{OC} = 0.63 K_{OW}$ (33) except for DDT and the PCBs. The measured adsorption $\log K_{OC}$ values of the more hydrophobic compounds in Table 2, DDT and the PCBs, are consistently lower than expected. Other researchers have reported similar results for such highly hydrophobic compounds, particularly the PCBs (32, 35, 36). The K_{OC} values reported by these authors are similar to the values found for the irreversible fraction, as will be discussed below. Similar K_{OC} values may reflect a common mechanism, but more work is needed with both laboratory and field samples in order to generalize about these important classes of compounds.

Maximum Irreversible Capacities q_{\max}^{irr} . Among the data listed in Table 2, q_{\max}^{irr} is probably the most difficult quantity to measure. Experimentally, q_{\max}^{irr} has to be measured at the end of all experiments since the analysis is destructive. The difficulties of quantitatively extracting the resistant fraction from soil have previously been addressed (3, 37, 38). For Naph, Phen, and Cl₄-PCB experiments, q_{\max}^{irr} values measured after solvent extraction agree with the expected concentration values based upon calculated mass balance [see the above discussion and Kan et al. (5)]. For the Cl₂-PCB experiment, part of the extracting solvent was accidentally spilled during the experiment, the resulting q_{\max}^{irr} measured in the solvent extract was 4.3 $\mu\text{g/g}$ (measured

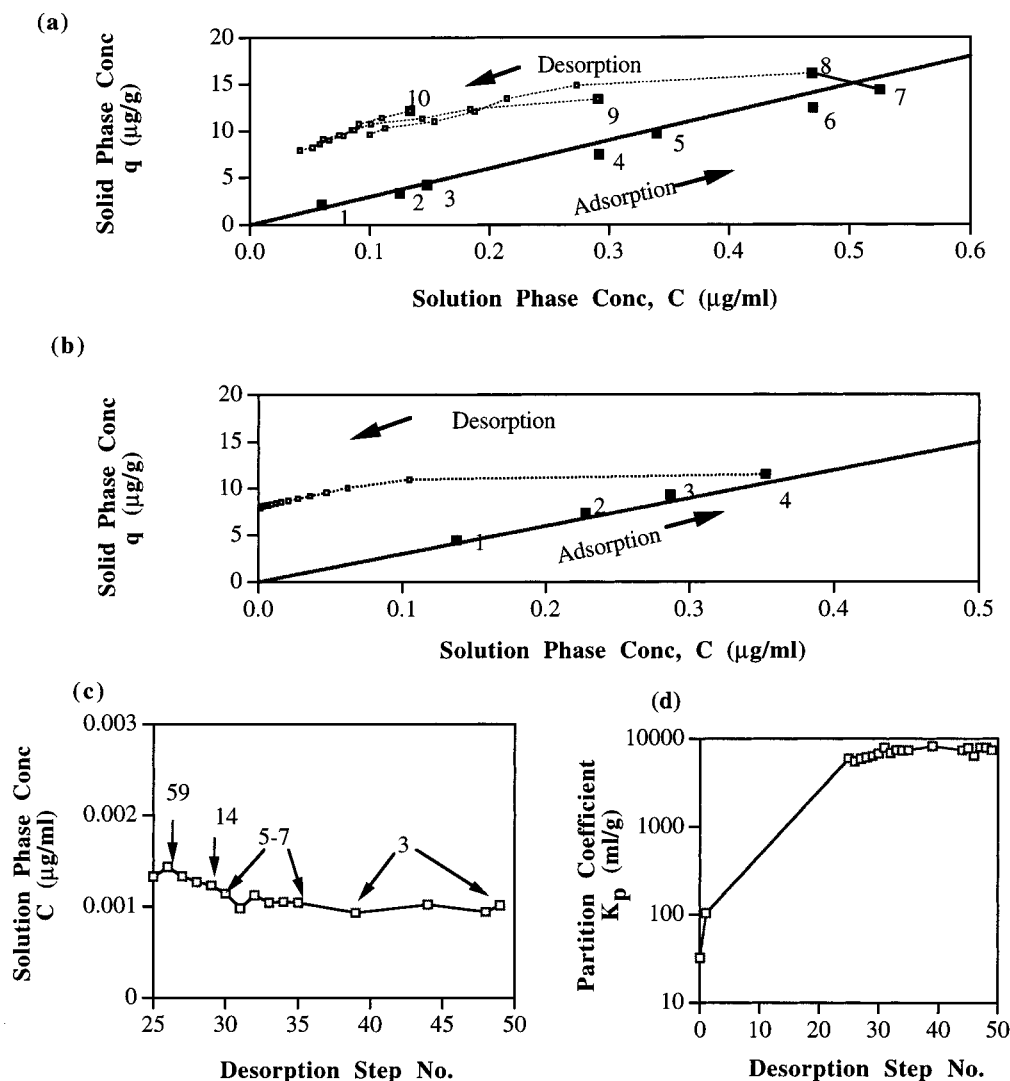


FIGURE 1. Plot of adsorption and desorption of Phen from Lula sediment. (a) Plot of the solid versus solution phase concentrations of exp. P-2, where three adsorption/desorption cycles are conducted. The numbers next to the symbols indicate the adsorption step number. (b) Plot of the solid versus solution phase concentrations of exp. P-4, where four adsorptions were followed by 49 desorption steps. (c) Plot of the solution phase Phen concentration versus desorption steps numbers 25–49 following adsorption no. 4 in panel b, above. The numbers indicate the equilibrium time (days) used for the desorption step. (d) Plot of the desorption partition coefficients (K_p) versus desorption step no., as in panel c.

by both GC and scintillation counting), which is equivalent to 73% of that ($5.9 \mu\text{g/g}$) calculated from the change in solution-phase mass balance. In the Cl_2 -Ben experiment, methylene chloride extraction yielded a solid-phase concentration of $44 \mu\text{g/g}$ (by scintillation counting) and $52 \mu\text{g/g}$ (by GC analysis) versus $37 \mu\text{g/g}$ calculated from the changes in solution-phase mass balance, which is the largest variation observed. However, this experiment used both ^{12}C and ^{14}C isomers in the five cycles of adsorption/desorption over 120 individual experiments, which complicates the data analysis. Several $q_{\text{max}}^{\text{irr}}$ values listed in Table 2 are calculated values based on the corresponding solution phase concentrations and the data were not confirmed with solvent extraction.

Discussion

Irreversible Adsorption $q_{\text{max}}^{\text{irr}}$ and $K_{\text{OC}}^{\text{irr}}$. The observed maximum irreversible capacity ($q_{\text{max}}^{\text{irr}}$) developed in the laboratory should account for the observations of resistant fractions reported in the literature. If this is the case, literature reported resistant fractions should be equal to (within experimental error) or less than the laboratory determined

maximum values. Values of $q_{\text{max}}^{\text{irr}}$ ($\mu\text{g/g}$) determined in this study are reported in Table 2 and are plotted in Figure 2 along with numerous contaminant concentrations measured in field contaminated samples from both this study and literature. The Utica sediments contained a number of polycyclic aromatic hydrocarbons (PAHs): $1.0 \mu\text{g/g}$ naphthalene, $1.6 \mu\text{g/g}$ acenaphthene, $10.1 \mu\text{g/g}$ acenaphthylene, $5.5 \mu\text{g/g}$ fluorene, $12.3 \mu\text{g/g}$ phenanthrene, $8.9 \mu\text{g/g}$ anthracene, $19.4 \mu\text{g/g}$ fluoranthene, and $23.7 \mu\text{g/g}$ pyrene. The Lake Charles sediment contained $4.0 \mu\text{g/g}$ 1,3-dichlorobenzene, $18.6 \mu\text{g/g}$ 1,4-dichlorobenzene, $0.5 \mu\text{g/g}$ 1,2,4-trichlorobenzene, $2.7 \mu\text{g/g}$ hexachlorobutadiene, and $101.9 \mu\text{g/g}$ hexachlorobenzene. As expected, nearly all literature reported resistant fraction concentrations on soil (11, 19–21, 39–42) fall below the laboratory determined $q_{\text{max}}^{\text{irr}}$ curve in Figure 2.

To model the $q_{\text{max}}^{\text{irr}}$ values, it is proposed that the irreversible compartment is a consequence of an interaction of the hydrocarbon with the organic matter of the sediment, in some manner. There are two aspects of the interaction, the amount of compound in the water and the energy per

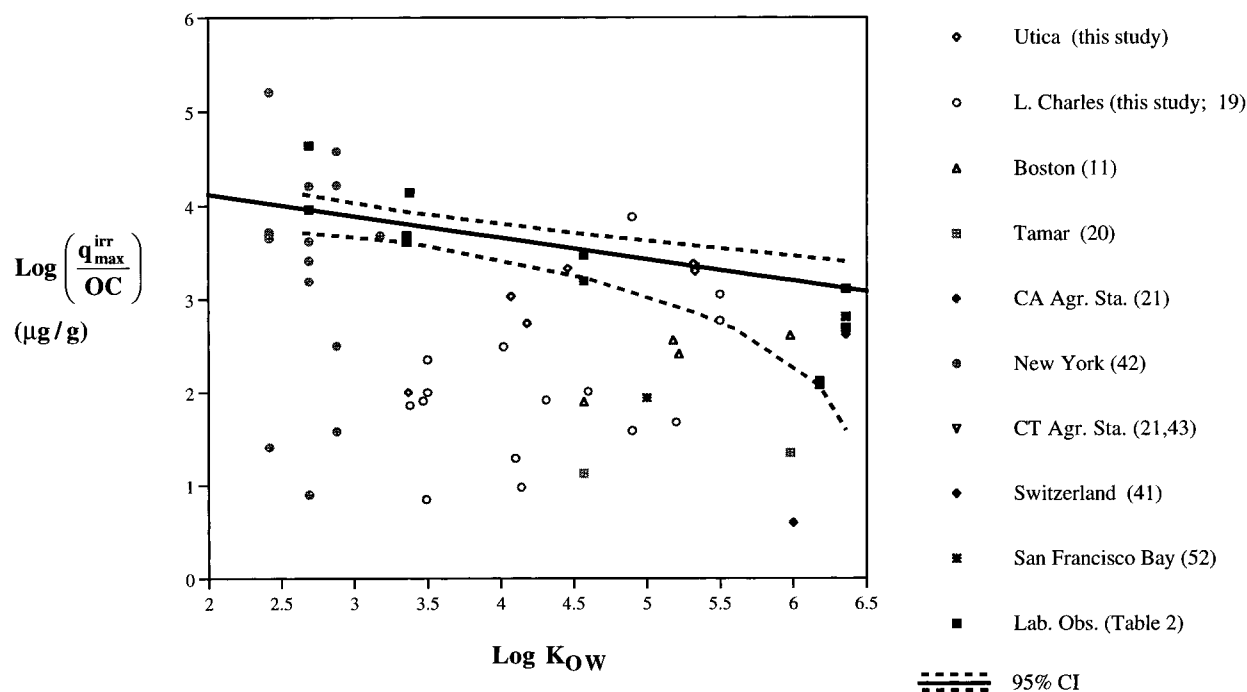


FIGURE 2. Plot of the OC normalized solid-phase chemical concentration that resists desorption versus K_{OW} . The solid squares are laboratory observed maximum capacities ($q_{max}^{irr}/OC, \mu\text{g/g}$) of various chemicals on Lula and Dickinson Bayou sediments. The other symbols are OC normalized solid-phase concentration ($q/OC, \mu\text{g/g}$) in historically contaminated field sediments of various locations.

interaction. Therefore, the following semiempirical model is proposed to represent the q_{max}^{irr} :

$$\begin{aligned}
 q_{max}^{irr} \text{ (mg/g)} &= \\
 &a \times OC(C_{aq}^{sat}) \exp \left\{ \frac{-\Delta G_{ads}^{irr}(j/A^2)HSA(A^2/\text{molecule})}{RT/N_{Av}} \right\} \\
 &= 0.044OC(C_{aq}^{sat}) \exp(0.048HSA) \quad (3) \\
 &\approx 37765OC \times K_{OW}^{-0.23}
 \end{aligned}$$

where ΔG_{ads}^{irr} represents the free energy of adsorption per unit area of molecule (determined by curve fitting), HSA (43) is the hydrophobic surface area ($A^2/\text{molecule}$) and can be related to $\log K_{OW}$, R is the gas constant ($\text{J mole}^{-1} \text{K}^{-1}$), T is temperature (K), N_{Av} is Avogadro's number, and C_{aq}^{sat} ($\mu\text{g/mL}$) is the aqueous concentration at saturation and a is a constant. Using a nonlinear least-squares program (PSI-Plot 3), ΔG_{ads}^{irr} for Naph is found to be -18.3 kJ/mol , which is similar to the free energy of stabilization due to the irreversible adsorption previously reported by the authors (5). This excess free energy is also similar in magnitude to the excess free energy of Naph adsorption to soil (44). Therefore, the interaction between the chemical and the irreversible compartment is probably a result of nonspecific van der Waals type interactions.

Interestingly, the aqueous phase concentrations in equilibrium with q_{max}^{irr} for Naph and DDT are similar in magnitude even though their aqueous solubilities differ by about 4 orders of magnitude and their K_{OW} values differ by 3 orders of magnitude. Similarly, Chen (45) observed the solution phase Cl_2 -Ben and hexachlorobenzene concentrations at equilibrium with the Lake Charles sediment to be nearly identical. It is also surprising to find that compounds as different as Tol and DDT share a relatively constant K_{OC}^{irr} value. The K_{OC}^{irr} values for all experiments are relatively constant with a mean $\log K_{OC}^{irr}$ of 5.53 and a standard

deviation of 0.48. This is consistent with numerous literature reported field observations that the K_{OC} values of the resistant phase are nearly constant, or of lesser dependence on K_{OW} than would be expected (24, 25, 27).

There are several plausible hypotheses for such observations. For example, if the chemical in the irreversible compartment forms an organic complex with the organic colloids in the soil organic matter (46, 47), the physical-chemical nature of the adsorbate would be masked by the complex. Desorption of the adsorbate would be predominantly related to the desorption properties of the organic complex. Some preliminary testing of this concept with dialysis experiments has shown that such an organic complex probably exists, but more research is needed. A second hypothesis is that the larger chemical molecules are less stable than the smaller chemical molecules in the irreversible compartment due to, e.g., the proximity of electrostatic forces, hydrogen bonding, or steric effects in the irreversible compartment. Consequently, the more hydrophobic compounds, e.g., DDT, are less stable than Tol in the irreversible compartment, and this reduction in stability (i.e. increase in activity coefficient) might parallel the corresponding values in solution and the ratio would be nearly constant. A third possibility is that the irreversibility is originated from condensation (filling) into capillaries or ink-bottle pores in the solid phase. A cylindrical capillary diameter of about 5–50 Å can be estimated with the desorption data listed in Table 2 and the Kelvin equation (16). Each of these mechanistic explanations has shortcomings and will be discussed elsewhere when more testing has been completed.

Irreversible Adsorption Isotherm. Three generalizations can be made from the results. First, for each compound and sediment combination, there exists a maximum solid-phase irreversible capacity (q_{max}^{irr}) and this maximum can be predicted with commonly available parameters (eq 3). Second, K_{OC}^{irr} is approximately a constant ($10^{5.53} \text{ mL/g}$) for different chemicals and sediment types. Third, the irreversible compartment can be filled stepwise, depending on the original contaminant concentration. The irreversible com-

partment can be filled in one step if the solution-phase concentration at equilibrium is greater than about one-half of the aqueous solubility (C_{aq}^{sat}).

Considering the above observations and previous results published by the authors (2-5), a biphasic model of adsorption is proposed:

$$q \text{ (}\mu\text{g/g of sediment)} = q^{rev} \text{ (}\mu\text{g/g of sediment)} + q^{irr} \text{ (}\mu\text{g/g of sediment)} \quad (4)$$

where q ($\mu\text{g/g}$) represents the total concentration of adsorbed compound in the solid phase, q^{rev} ($\mu\text{g/g}$) represents the concentration of adsorbed compound in the solid phase that can participate in labile or reversible partitioning, and q^{irr} ($\mu\text{g/g}$) represents the concentration of adsorbate that is sorbed in the second, or irreversible, compartment. Sorption to the reversible compartment has been shown to be well represented by a commonly used linear isotherm, $q^{rev} = K_{OC} \times OC \times C$. Since the q^{irr} portion has a well-delineated maximum for each compound and sediment combination (see ref 5 and the discussion related to eq 3, above), a Langmuirian-type sorption isotherm is derived to represent this portion of the sorption. Substituting the linear and Langmuirian portions to eq 4, the overall sorption can be represented by the following equation:

$$q = K_{oc} \times OC \times C + \frac{K_{OC}^{irr} \times OC \times q_{max}^{irr} \times fC}{q_{max}^{irr} f + K_{OC}^{irr} \times OC \times C} \quad (5)$$

where q_{max}^{irr} is defined in eq 3 and K_{OC}^{irr} (mL/g) is analogous to K_{oc} in eq 2, but for the irreversible compartment. f ($0 \leq f \leq 1$) is the fraction of the irreversible compartment that is filled at the time of exposure and can be assumed equal to 1 when the exposure concentration is greater than about one-half the aqueous solubility, which is probably the case in most point source contamination. The functional form of the second term on the right-hand side of eq 5 can be rearranged to a more commonly expressed Langmuir isotherm $\{bQ^2C/(1 + bC)\}$, by dividing the numerator and denominator by $q_{max}^{irr}f$ and setting $Q = q_{max}^{irr}f$. When the aqueous concentration, C ($\mu\text{g/mL}$), is relatively large, the second term reduces to a constant, q_{max}^{irr} . Similarly, when C is relatively small, the second term reduces to $K_{OC}^{irr} \times OC \times C$. If the data from the above isotherm are fitted as if it were a Freundlich isotherm with $q = K_f C^n$, the value of n will vary from about 0.50 to 0.99 [similar to reported values, (48)]. It will be seen below that eq 5 represents a wide range of laboratory and field data.

Using the proposed irreversible adsorption isotherm (eq 5), we are able to match nearly all laboratory data using the values listed in Tables 2. Figure 3 is a plot of seven compounds adsorption desorption data, which was summarized in Table 2. The data were fitted with the reversible (dashed lines) and irreversible isotherms (solid and dotted lines eq 5), where the symbols are the experimental data and the lines are the predictions. Details of the six Naph experimental procedures have been discussed in previous papers (2, 5). These six Naph experiments (Figure 3a) were done at different initial Naph concentrations, hence the irreversible compartments were filled to different degrees, f , as noted in the caption. The solid and dotted lines are model predictions at $f = 1.0, 0.5, 0.25, 0.132, 0.084, \text{ and } 0.031$, respectively; in each case, q_{max}^{irr} in eq 5 is multiplied by f . Most of the data fit model predictions, except in the very low concentration region ($<0.01 \mu\text{g/mL}$) where actual desorption appears to be even more resistant than the model predicts. In Figure 3, panels b and c, two cycles of desorption data for Tol and Cl_2 -Ben at different f values are included for

comparison. Similarly, the data fit the model very well except for some of the lowest concentration regions. Note that the effect of irreversible adsorption is more pronounced for lower K_{OW} compounds (e.g., Tol, Cl_2 -Ben, Naph, and Phen), where the differences between reversible and irreversible adsorption predictions are as much as 3 orders of magnitude (e.g., for Tol). The effect of irreversible adsorption is less pronounced for highly hydrophobic compounds (e.g., PCBs, high molecular weight PAHs, and DDT). McGroddy et al. (11) observed similar deviation between the low K_{OW} compounds (Phen and pyrene) and high K_{OW} compounds ($2,2',4,5,5'$ - Cl_5 -PCB and $2,2',3,4,4',5'$ - Cl_6 -PCB). They attributed the observations to specific affinity of PAHs to ubiquitous soots.

The reversible and irreversible sorption models should bracket most literature data. In Figure 4, the sediment (OC normalized) and water-phase concentrations of selected literature data are plotted ($f = 1$). The symbols are for different compounds and their location at the reported (q, C) value. The literature data are those reported for Boston Harbor (11) and Bayou d'Inde, Lake Charles, LA sediments (19, 45). The chemicals in Boston Harbor are Phen, pyrene, Cl_5 - and Cl_6 -PCB. The chemicals in Lake Charles are predominantly chlorinated benzenes and hexachlorobutadiene. The irreversible model predictions (solid lines) are plotted at $\log K_{OC} = 2.0, 3.0, 4.0, 5.0, 6.0, \text{ and } 7.0$ with $\log K_{OC}^{irr} = 5.53$ in all cases. The shaded area on either side of the irreversible isotherm represents the laboratory measured standard deviation (± 0.48) of $\log K_{OC}^{irr}$ (see Table 2). The irreversible isotherms with $\log K_{OC}$ less than 5.53 converge at the low concentration region of the curves. The corresponding reversible model predictions at different $\log K_{OC}$ values are also plotted (dashed lines) for comparison.

The plateau at $q \approx q_{max}^{irr} = 10^{3.8} \mu\text{g/g OC}$ corresponds to $K_{OC} = 10^3$ and $K_{OW} = 10^{3.36}$ (eq 3) and is approximately constant (Figure 2) for a range of compounds, but if the primary interest is this region of the isotherm, the value of q_{max}^{irr}/OC should be adjusted slightly (eq 3) for each $\log K_{OW}$. For compounds with $\log K_{OC}$ less than 5.53, the differences between the reversible and irreversible model prediction become more significant with lower K_{OC} values. For compounds with $\log K_{OC}$ greater than $\log K_{OC}^{irr}$, the predicted effect of K_{OC}^{irr} on the net adsorption is negligible. Many researchers have reported that compounds with larger K_{OC} values are difficult to study quantitatively (32) and will be the focus of more research by the present authors and probably by others.

For every field datum point in Figure 4, the irreversible isotherm, eq 5, comes closer to predicting the observed adsorption than the reversible isotherm alone. Both PAHs and some of the chlorinated compound data lie slightly to the left and above the irreversible isotherm region, indicating that the chemicals in these sediments are more resistant to desorption than predicted from the laboratory derived K_{OC}^{irr} value. A better empirical fit to the data plotted in Figure 4 and other similar data would be obtained by using $K_{OC}^{irr} = 10^6 - 10^{6.5}$, suggesting that the laboratory derived K_{OC}^{irr} value might systematically underestimate the irreversible adsorption which takes place with natural sediments. Also, this apparent added resistance to desorption might be a consequence of a kinetic resistance to desorption at these extremely low concentrations. Such kinetic resistance to desorption might be a consequence of either the flushing or flow rate in the field relative to the desorption rate and amount (see modeling below) or a consequence of the way the samples were handled. Kinetic desorption would tend to move the datum to the right and downward toward the isotherm line with a slope $= -I_{sw}$, where I_{sw} is the ratio of mass of solid to volume of water ($\text{g of sediment/mL of water}$). If field measurements occur to the right of and below the predicted irreversible isotherm, this might suggest the

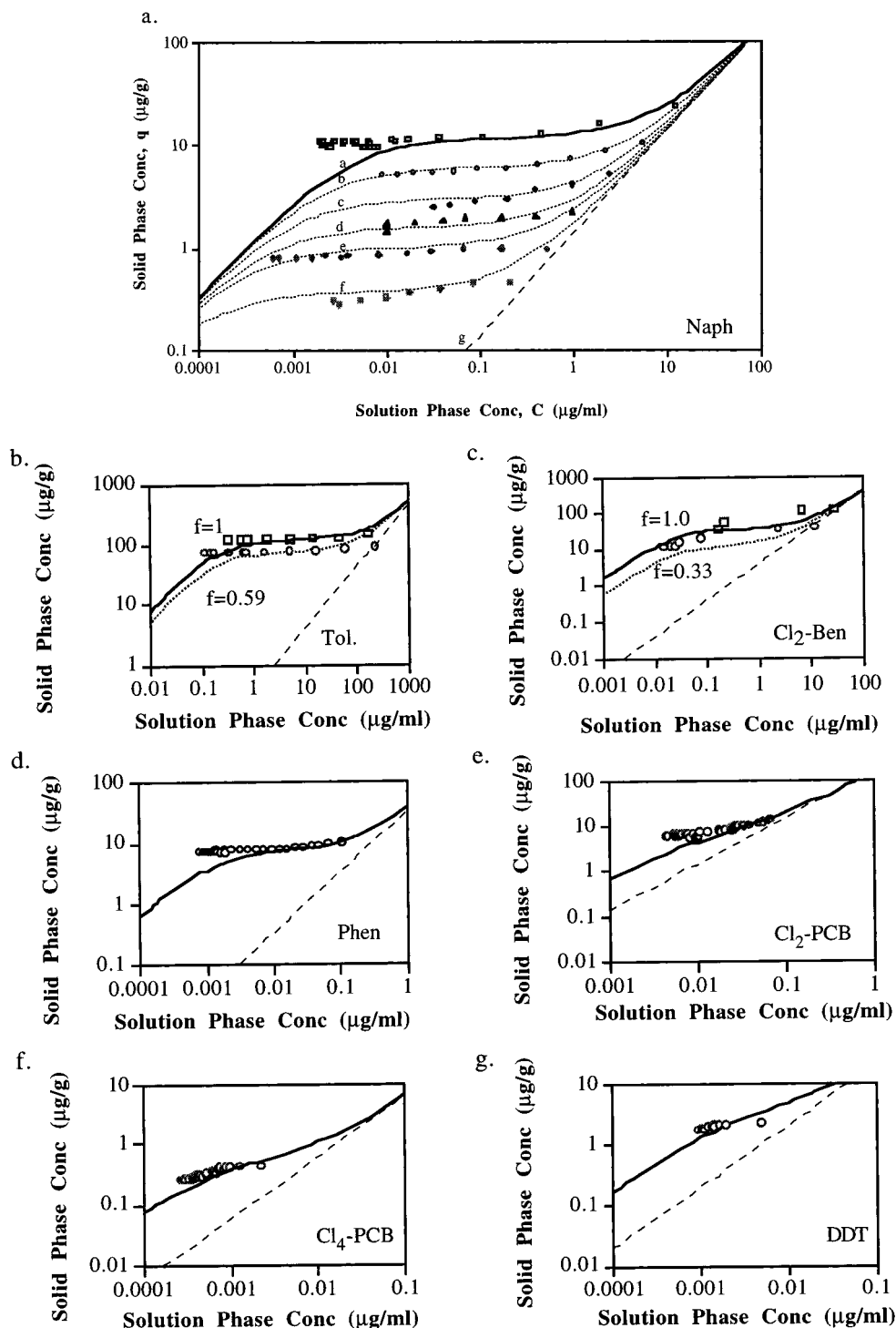


FIGURE 3. Plot of the irreversible adsorption isotherm solid phase versus solution phase concentrations. The symbols are the experimental desorption data with Lula sediment. The six Naph experiments are differed in the fraction of irreversible compartment filled, with $f = 1.0, 0.50, 0.25, 0.132, 0.0837,$ and 0.0309 , respectively (see exp N-4, N-2, N-1, 1d, 18d, and 16d in refs 2 and 7). In Tol and $\text{Cl}_2\text{-DCB}$ plots, two cycles of adsorption/desorption data were plotted and the corresponding f values are given. In the other experiments, the last cycle of desorption data was plotted at $f = 1$. The lines are the corresponding prediction with the irreversible and reversible isotherms (eq 5), where the solid line is for $f = 1$, dotted line is for $0 < f < 1$, and dashed line is for $f = 0$ (reversible model).

presence of active colloidal partitioning (27, 49, 50). Equation 5 can be modified to include the effect of colloids on partitioning by dividing both terms on the right-hand side of eq 5 by $1 + r_{cw}K_c$, where r_{cw} (g/mL) is the ratio of the mass of colloid to the volume of water and K_c (mL/g) is the partitioning coefficient for adsorption to the colloid. Either micelles from a surfactant or dissolved organic matter would be treated in the same way. The hexachlorobenzene solid-

phase concentration in Lake Charles sediment is unusually high. It is suspected that a small amount of a separate hexachlorobenzene phase might exist in the solid; the presence of a separate contaminant phase in the solid would in general be indicated by a high value of q . The model predictions are in reasonable agreement with the PCB data, even though these compounds are highly hydrophobic with log K_{OW} values of 6.3 and 6.8. Numerous other field data (24,

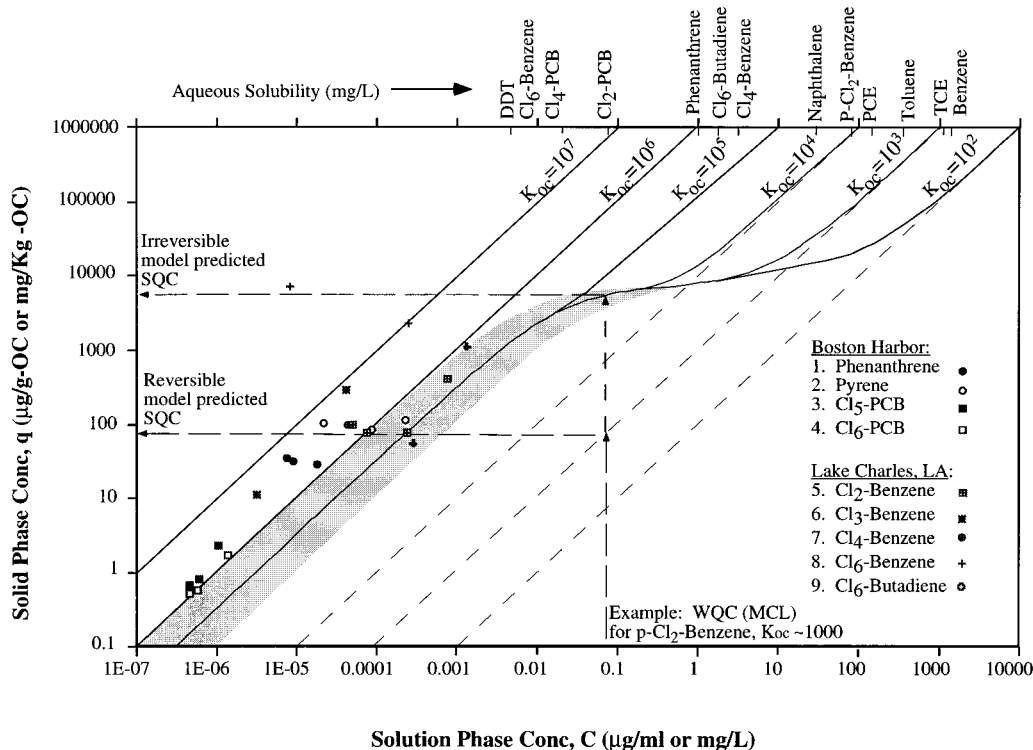


FIGURE 4. Plot of the solid-phase concentration ($\mu\text{g/g-OC}$) versus the aqueous phase concentration ($\mu\text{g/mL}$) of model predictions and literature reported data. The solid curves are the irreversible isotherm for compounds with $\log K_{oc}$ values ranging from 2 to 7. The shaded area is the predicted interval for $\log K_{oc} = 3$ and $\log K_{oc}^{irr} = 5.53 \pm 0.48$. The dashed 45° lines are the equilibrium partitioning isotherms for compounds with $\log K_{oc} = 2-7$. The phenanthrene, pyrene penta- and hexachlorobiphenyl data are from McGroddy et al. (17), and chlorinated benzenes and hexachlorobutadiene data are from Pereira et al. (19). Also included are the chlorinated benzenes and hexachlorobutadiene data from Chen (46). The "plus sign inside a square" data points are the *p*-dichlorobenzene concentration observed at Bayou d'Inde, Lake Charles, LA (19, 46). The dashed arrows point to an example where the sediment quality criteria (SQC) values are estimated with either the reversible or the irreversible models and the drinking water standard (MCL) of *p*-dichlorobenzene.

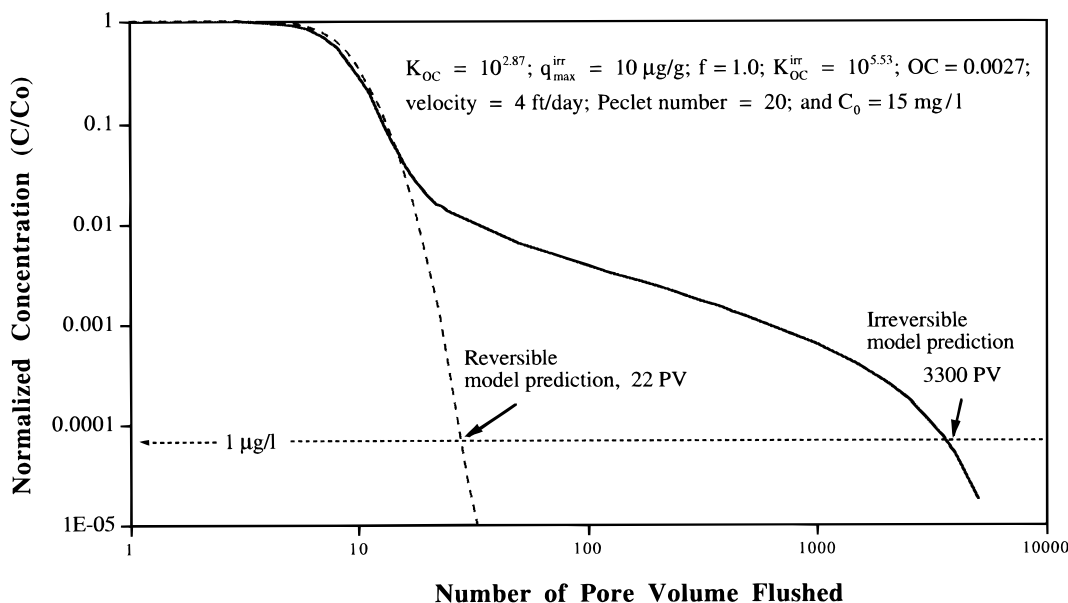


FIGURE 5. Plot of the normalized concentration versus flush-out pore volumes to simulate the cleanup of a contaminated site with water and assumed reversible and irreversible adsorption isotherms. The simulations are calculated with the 1-D advective-dispersive transport model of Kool and Parker (54), incorporated with the two adsorption isotherms. The model parameters are shown in the plot. The model predicts that 22 pore volumes are required to cleanup this site using the reversible model, while over 3300 pore volumes are required to cleanup when the chemical is adsorbed irreversibly.

27, 51, 52) have been compared with the irreversible model with similar agreement as depicted in Figure 4.

Implications for Sediment Quality Criteria. The U.S. EPA has proposed sediment quality criteria (SQC) to ensure

that the sediment-phase contaminant concentrations are within acceptable limits for the protection of both aquatic organisms and human health. The proposed SQC is based on the equilibrium (reversible) partitioning of the sediment

with a final chronic water quality criterion value. This approach has great scientific and economic support. As discussed above, a SQC based on the reversible partitioning model has the potential to overestimate the desorption and the associated risk to the environment. This is illustrated in Figure 4 with the *p*-dichlorobenzene data reported in Lake Charles sediment (19). Considering the water quality criterion (which is assumed to be equal to the drinking water standard, MCL) for *p*-dichlorobenzene and a reversible model, all of the sediment samples (those points marked with a plus sign inside a square) exceed the sediment quality criteria (SQC) and would require cleanup. However, the actual pore water concentration is about 3 orders of magnitude lower than the MCL and is probably not going to adversely affect the environment. If the irreversible adsorption model were adopted, the sediment would not exceed SQC and could be left alone. That is, the present model predicts that about one hundred times more dichlorobenzene could be left on the sediment with no increase in adverse health or environmental effects. Similar results are predicted for other compounds with similar or smaller K_{OC} values.

Implication to Contaminant Transport and Remediation. The proposed irreversible adsorption isotherm model has significant implications in contaminant fate, transport, and remediation. This isotherm can be easily incorporated into fate and transport models using the derivative of the irreversible isotherm (eq 6):

$$\frac{dq}{dC} = K_{oc} \times OC + \frac{K_{OC}^{irr} \times OC (q_{max}^{irr} f)^2}{(q_{max}^{irr} f + K_{OC}^{irr} \times OC \times C)^2} \quad (6)$$

In Figure 5, the volumes of water required to remediate a site are simulated by assuming a reversible (dashed line) and an irreversible isotherm (solid line). The simulations were done using the one-dimensional advective dispersive transport code of Kool and Parker (53) with these assumptions:

$$K_{OC} = 10^{2.87} \text{ mL/g}; K_{OC}^{irr} = 10^{5.53} \text{ mL/g}$$

$$q_{max}^{irr} = 10 \text{ mg/g}; OC = 0.0027$$

$$\text{velocity} = 4 \text{ ft/day}; \text{pecllet number} = 20$$

$$C_0 = 15 \text{ mg/L}; f = 1$$

The cleanup objective was 0.001 $\mu\text{g/mL}$ in each case. The reversible isotherm predicts that the site can be cleaned up in less than 22 pore volumes, while the irreversible isotherm predicts that a cleanup volume of over 3300 pore volumes would be required to bring the concentration down to below 0.001 $\mu\text{g/mL}$. Apparently, the simple extraction method of pump and treat cannot economically remediate the resistant fraction. Some limited data have shown that extraction of this resistant fraction is also difficult with surfactant and cosolvent flushing (3, 42, 54). In this paper, it has been shown that pollutants would not be released from sediments in any significant concentration. If these contaminants in sediments will not be released biologically, they would be of little practical concern and could be left in place.

Acknowledgments

This research has been conducted under the auspices of the South & Southwest Hazardous Substance Research Center with funding provided by the Office of Exploratory Research of the U.S. Environmental Protection Agency. We also thank Dr. C. R. Demas of U.S. Geological Survey Louisiana District for assistance in collecting Lake Charles sediments.

Literature Cited

- (1) Parker, J. C.; Genuchten, M. T. v. *Determining Transport Parameters from Laboratory and Field Tracer Experiments*; Virginia Agricultural Experiment Station, 1984.

- (2) Kan, A. T.; Fu, G.; Tomson, M. B. *Environ. Sci. Technol.* **1994**, *28*, 859–867.
- (3) Fu, G.; Kan, A. T.; Tomson, M. B. *Environ. Chem. Toxicol.* **1994**, *13*, 1559–1567.
- (4) Hunter, M. A.; Kan, A. T.; Tomson, M. B. *Environ. Sci. Technol.* **1996**, *30*, 2278–2285.
- (5) Kan, A. T.; Fu, G.; Hunter, M. A.; Tomson, M. B. *Environ. Sci. Technol.* **1997**, *31*, 2176–2185.
- (6) Adamson, A. W. *Physical Chemistry of Surfaces*, 5th ed.; J. Wiley & Sons, Inc.: New York, 1990.
- (7) Bailey, A.; Cadenhead, D. A.; Davies, D. H.; Everett, D. H.; Miles, A. J. *Trans. Faraday Soc.* **1971**, *67*, 231.
- (8) Burgess, C. G. V.; Everett, D. H.; Nuttall, S. *Pure Appl. Chem.* **1989**, *61*, 1845–1852.
- (9) Burgos, W. D.; Novak, J. T.; Berry, D. F. *Environ. Sci. Technol.* **1996**, *30*, 1205.
- (10) Weber, W. J., Jr.; Huang, W. *Environ. Sci. Technol.* **1996**, *30*, 881.
- (11) McGroddy, S. E.; Farrington, J. W.; Gschwend, P. M. *Environ. Sci. Technol.* **1996**, *30*, 172–177.
- (12) Xing, B.; Pignatello, J. J.; Gigliotti, B. *Environ. Sci. Technol.* **1996**, *30*, 2432–2440.
- (13) Carroll, K. M.; Harkness, M. R.; Bracco, A. A.; Balcarcel, R. R. *Environ. Sci. Technol.* **1994**, *28*, 253–258.
- (14) Pignatello, J. J.; Xing, B. *Environ. Sci. Technol.* **1996**, *30*, 1–10.
- (15) Farrell, J.; Reinhard, M. *Environ. Sci. Technol.* **1994**, *28*, 63–72.
- (16) Ruthven, D. M. *Principles of adsorption and adsorption processes*; Wiley: New York, 1984.
- (17) Crank, J. *The Mathematics of Diffusion*, 2nd ed.; Clarendon Press: Oxford, 1975.
- (18) Wu, S.-C.; Gschwend, P. M. **1988**, *24*, 1373–1383.
- (19) Pereira, W. E.; Rostad, C. E.; Chiou, C. T.; Brinton, T. I.; Barbar, L. B., II. *Environ. Sci. Technol.* **1988**, *22*, 772–778.
- (20) Readman, J. W.; Mantoura, R. F. C. *Sci. Total Environ.* **1987**, *66*, 73–94.
- (21) Steinberg, S. M.; Pignatello, J. J.; Sawhney, B. L. *Environ. Sci. Technol.* **1987**, *21*, 1201–1208.
- (22) Hutchins, S. R.; Tomson, M. B.; Ward, C. H. *Environ. Toxicol. Chem.* **1983**, *2*, 195–216.
- (23) Beck, A. J.; Wilson, S. C.; Alcock, R. E.; Jones, K. C. *Crti. Rev. Environ. Sci. Technol.* **1995**, *25*, 1–43.
- (24) Pearson, R. F.; Hornbuckle, K. C.; Eisenreich, S. J.; Swackhamer, D. L. *Environ. Sci. Technol.* **1996**, *30*, 1429–1436.
- (25) Thibodeaux, L. J.; Valsaraj, K. T.; Reible, D. D. *Water Sci. Technol.* **1993**, *28*, 215–221.
- (26) Burgess, R. M.; McKinney, R. A.; Brown, W. A. *Environ. Sci. Technol.* **1996**, *30*, 2556–2566.
- (27) Baker, J. E.; Capel, P. D.; Eisenreich, S. J. *Environ. Sci. Technol.* **1986**, *20*, 1136–1143.
- (28) Chandra, S. D.; Ward, C. H.; Hughes, J. B. *Hazard. Waste Hazard. Mater.* **1996**, *13*, 375–385.
- (29) Wilson, J. T.; Enfield, C. G.; Dunlap, W. J.; Cosby, R. L.; Foster, D. A.; Baskin, L. J. *Environ. Qual.* **1981**, *10*, 501–506.
- (30) Demas, C. R.; Demcheck, D. K. *Remobilization of organic compounds from bottom material collected from Bayou D'Inde, Louisiana, upon exposure to differing ionic-strength waters*; U.S. Geol. Survey-Water Resources Investigation Report, 1988.
- (31) Demas, C. R.; Demcheck, D. K. *Fate and transport of organic compounds and trace elements in the lower Calcasieu River, Louisiana*; U.S. Geological Survey, 1988.
- (32) Schwarzenbach, R. P.; Gschwend, P. M.; Imboden, D. M. *Environmental Organic Chemistry*; J. Wiley & Sons, Inc.: New York, NY, 1993.
- (33) Karickhoff, S. M.; Brown, D. S.; Scott, T. A. *Water Res.* **1979**, *13*, 241–248.
- (34) Karickhoff, S. W. *J. Hydraul. Eng.* **1984**, *110*, 707–735.
- (35) Axelman, J.; Broman, D.; Naf, C. *Environ. Sci. Technol.* **1997**, *31*, 665–669.
- (36) Chiou, C. T.; Schmedding, D. W.; Manes, M. *Environ. Sci. Technol.* **1982**, *16*, 4–10.
- (37) Huang, L. Q.; Pignatello, J. J. *J. Assoc. Off. Anal. Chem.* **1990**, *73*, 443–446.
- (38) Pignatello, J. J. *Environ. Toxicol. Chem.* **1989**, *9*, 1107–1115.
- (39) Spencer, W. F.; Singh, G.; Taylor, C. D.; LeMert, R. A.; Clith, M. M.; Farmer, W. J. *J. Environ. Qual.* **1996**, *25*, 815–821.
- (40) Marcomini, A.; Capel, P. D.; Lichtensteiger, T.; Brunner, P. H.; Giger, W. *J. Environ. Qual.* **1988**, *18*, 523–528.
- (41) Pavlostathis, S. G.; Geeyerapuram, N. M. *Environ. Sci. Technol.* **1992**, *26*, 532–538.
- (42) Pignatello, J. J. *Environ. Toxicol. Chem.* **1990**, *9*, 1117–1126.
- (43) Sabljic, A. *Environ. Sci. Technol.* **1987**, *21*, 358–366.

- (44) Podoll, T.; Irwin, K. C.; Parish, H. J. *Chemosphere* **1989**, *18*, 2399–2412.
- (45) Chen, W. *Sorption and desorption of hydrocarbons to and from historically contaminated Lake Charles sediments*; M. S., Rice University, 1997.
- (46) Schulten, H.-R.; Schnitzer, M. *Soil Sci.* **1997**, *162*, 115–130.
- (47) Devitt, E. C.; Wiesner, M. R. *Environ. Sci. Technol.* **1998**, *32*, 232–237.
- (48) Huang, W.; Weber, W. J., Jr. *Environ. Sci. Technol.* **1997**, *31*, 2562–2569.
- (49) Kan, A. T.; Tomson, M. B. *Environ. Toxicol. Chem.* **1990**, *9*, 253–263.
- (50) Gschwend, P. M. a. W. S. *Environ. Sci. Technol.* **1985**, *19*, 90–96.
- (51) Maruya, K. A.; Risebrough, R. W.; Horne, A. J. *J. Environ. Sci. Technol.* **1996**, *30*, 2942–2947.
- (52) Hornbuckle, K. C.; Achman, D. R.; Eisenreich, S. J. *Environ. Sci. Technol.* **1993**, *27*, 87–98.
- (53) Kool, J. B.; Parker, J. C.; Zelazny, L. W. *Soil Sci. Soc. Am. J.* **1988**, *53*, 1347–1355.
- (54) Kan, A. T.; Hunter, M. A.; Fu, G.; Tomson, M. B. *SPE Production and Facilities*, August 1997; pp 153–157.

Received for review July 3, 1997. Accepted December 12, 1997.

ES9705809